IJLESS (International Journal of Languages, Education and Social Sciences) Volume 31, Issue 03,
Publishing Date of the Paper: 30th June, 2023
An Indexed, Refereed and Peer Reviewed Journal with ISSN: 2278-3970
www.ijless.com

Exploring Temperature-Dependent Intermolecular Interactions: A Study of Piperidinium Based Ionic Liquid with 2-Methoxy Aniline

G V Gangadhara Rao[1*], Dr. M. Madhu[2]

[1]Lecturer in Physics, CSTS Government Kalasala, Jangareddigudem, Eluru District, AndhraPradesh, India
[2]Lecturer in Chemistry, CSTS Government Kalasala, Jangareddigudem, Eluru District, AndhraPradesh, India
**Corresponding Author: gangadhara.gurijala@gmail.com*

Abstract

In this experimental investigation, we conducted a study to determine the thermophysical properties of density (ρ) and speed of sound (U) for the aromatic aniline group, specifically 2-methoxy aniline, in a solution of piperidinium-based ionic liquid, namely 1-Butyl-1-methyl piperidinium tetra fluoroborate ([BMPip]BF_4), at different concentrations and temperatures ranging from 303.15K to 313.15K. Through our experiments, we obtained precise values for these properties and analyzed them to derive various thermodynamic acoustic parameters, including excess isentropic compressibility (K_S^E) and excess molar volume (V^E), which characterize specific and non-specific molecular interactions. Furthermore, our findings revealed significant interactions between [BMPip]BF_4 and 2-methoxy aniline at a temperature of 303.15K, surpassing any other higher temperatures in this combination. Additionally, we calibrated the partial molar volumes and partial isentropic compressibilities of both components, further supporting the presence of strong interactions within the [BMPip]BF_4 + 2-methoxy aniline combination at 303.15K.

Keywords: *Ionic Liquid, Partial isentropic compressibilites, Partial molar volumes.*

1. Introduction

The unique characteristics of Ionic Liquids (ILs) offer immense potential for various applications in the modern era [1]. Particularly, the thermophysical properties of ILs at room temperature play a pivotal role in numerous sectors, including industrial engineering, pharmaceutical manufacturing, and waste management treatment [2]. Through innovative approaches, binary fluid systems comprising ILs and organic solvents demonstrate versatile thermophysical properties. Notably, the molecular interactions occurring at specific concentrations of these binary fluids yield designer solvents based on ILs [3]. In this context, several groups of talented researchers have propelled the application of binary fluid combinations involving ILs in high-yield ionic liquid applications across various sectors [4]-[7]. In this research investigation, the authors conducted a comprehensive evaluation of a binary fluid mixture comprising IL of 1-butyl, 1-methyl piperidinium tetrafluoroborate ([BMPip]BF_4) and 2-methoxy aniline across a range of temperatures from 303.15K to 313.15K, under ambient atmospheric pressure conditions. The [BMPip]BF_4 IL, commonly employed in electrochemical energy applications such as lithium batteries and supercapacitors, was chosen for its desirable properties [8]-[11]. Additionally, due to the presence of the aniline group in the aromatic benzene of 2-methoxy aniline, it finds extensive use as a solvent in various physical and chemical fields. Furthermore, 2-methoxy aniline is utilized for corrosion prevention in oil refinery rigs. Consequently, the study of binary combinations involving the piperidinium group and the -NH_2 group has garnered significant attention. By analyzing fundamental properties such as density (ρ) and speed of sound (U), the researchers extracted thermodynamic excess features such as excess molar volume (V^E) and excess isentropic compressibility (K_S^E) of the binary fluids [12]-[13]. These fundamental features provide insights into the geometrical configurations and facilitate the development of structure-property correlations.

2. Material and Methods

Table 1: Specification of Source, CAS Number, Mass Fraction Purity and Further Purification

Name of the chemical	Source	CAS Number	Mass fraction purity	Further purification methods
2-methoxy aniline(2MCH)	HiMedia Laboratories, India	583-60-8	>99.70%	*GLPC
[BMPip]BF_4 (IL)	HiMedia Laboratories, India	345984-11-4	>99.70%	**Millipore

*Gas-Liquid partition chromatography carried through inert gas Ar.
**Impurities separation by filtration.

2.1 Specimen information

The 2-methoxyaniline (2MCH) underwent meticulous glass chromatography, ensuring precise separation and purification. The resulting fractions of 2MCH and ([BMPip]BF_4)(IL) were

meticulously documented and systematically arranged in Table 1, providing a comprehensive catalog of their properties.

Furthermore, Table 2 showcases an extensive compilation of crucial data, unveiling the density and speed of sound of the pure fluids of both the IL and 2MCH. This comprehensive tabulation empowers researchers and practitioners to delve into the intricate characteristics of these substances, offering invaluable insights for further analysis and experimentation. To establish the reliability and validity of the findings, the specimens obtained were meticulously cross-referenced with a range of esteemed and reputable articles. By correlating the obtained results with well-established scientific literature, the study ensures a solid foundation for its conclusions and strengthens its position within the existing body of knowledge[12],[14]-[15].

Table 2: Physical properties of pure component 2-methoxy aniline and IL with literature at specific temperatures

Sample	Parameter	Expt. /Lit.	Temperatures		
			303.15K	308.15K	313.15K
2MCH	ρ(kg.m^{-3})	Expt.	920.80	911.22	907.45
	ρ(kg.m^{-3})	Lit.	920.80[a]	911.22[a]	907.45[a]
	ρ(kg.m^{-3})	Lit.	920.84[b]	911.20[b]	907.44[b]
	U (m.s^{-1})	Expt.	1346.00	1324.30	1303.20
	U (m.s^{-1})	Lit.	1346.00[a]	1324.30[a]	1303.20[a]
	U (m.s^{-1})	Lit.	1346.00[b]	1324.20[b]	1303.80[b]
IL	ρ(kg.m^{-3})	Expt.	1410.54	1392.24	1374.56
	ρ(kg.m^{-3})	Lit.	1410.54[c]	1392.24[c]	1374.56[c]
	U (m.s^{-1})	Expt.	1484.22	1462.12	1443.22
	U (m.s^{-1})	Lit.	1484.22[c]	1462.12[c]	1443.22[c]

Here [a][12], [b][14], [c][15]

2.2 Evaluation Approach

The prepared dual liquids and pure liquids were dispensed into glass containers using a precision analytical balance (Mettler Toledo) with an accuracy of $\pm 10^{-11}$ kg. These containers were sealed tightly to prevent evaporation and absorption of moisture from the surroundings. The measured final mole fractions for the dual liquids have an uncertainty of less than ±0.0001. The dual liquids of the IL+2MCH system were prepared at specified concentrations, with mole fractions ranging from 0 to 1 in 12 consecutive steps. The temperature-dependent thermophysical properties such as density (ρ) and speed of sound (U) of the IL dual liquids were simultaneously determined using a vibrating-tube digital density and speed of sound analyzer at temperatures of 303.15K, 308.15K, and 313.15K. The entire apparatus includes a temperature-controlled bath regulated by an integrated Peltier thermostat with an accuracy of ±0.01K. As a result, the uncertainty values for the experimental density (ρ) and speed of sound (U) were below 0.01kg.m^{-3} and 0.5m.s^{-1} respectively.

3. Data Value and Validation

The experimentally calibrated thermo-physical fundamental features ρ and U were rearranged effectively for the binary fluid of IL+2MCH within temperature ranges 303.15K, 308.15K, and 313.15K. Figure 1 and Figure 2 graphically depict these features. The observed non-linear increasing trend suggests the existence of molecular interactions between the fluids[15]. This observation reveals that as the temperature increases, the interactions between molecules decreases. The eventual general expression is as follows:

$$Y^E = Y^r - Y^{id} --(1)$$

Here, $Y^E = V^E, K_s^E$ and $Y = \{V_m(molar\ volume), and\ Y = K_s(isentropic\ compressibility)\}$represent the real values of the fluids. Furthermore, the ideal component of thermodynamic acoustic parameters for molar volume and isentropic compressibility is represented by:

$$Y^{id} = x_1 Y_1 + (1 - x_1) Y_2 --(2)$$

In Equation (2), $x_1$is the mole fraction of component IL (1) with respect to 2MCH(2), while Y_1 and Y_2 represent the pure acoustic molar values of IL(1) and 2MCH(2), respectively. The isentropic compressibility $K_s$can be calculated using the equation:

$$K_s = \frac{1}{\rho U^2} --(3)$$

3.1 Redlich-Kister Polynomial Analysis

The conventional strategy for fitting the non-linear curve of attributes in binary fluids effectively involves Redlich-Kister polynomial regression[16]-[18], which incorporates legendre coefficients.

$$Y_{RK}^E = x_1(1 - x_1)\Sigma_{p=0}^{p=N} A_{p,T} L_p(2x_i - 1) --(4)$$

In this context, Y_{RK}^E represents the excess thermodynamic feature that can take any value (e.g., V^E, K_s^E). The standard deviation is also calibrated accordingly, considering M as the number of experimental values and N as the adjustable parameter.

$$\sigma(Y_{RK}^E) = \sqrt{\Sigma_{i=1}^{i=N} \frac{\left(Y_{i,exp} - Y_{i,cal}\right)^2}{M - N}} --(5)$$

These excess values are then analyzed using Redlich-Kister polynomial non-linear regression with legendre coefficients. The values of $A_{i,T}$(i=0,1,2,3) and their respective standard deviations are determined based on the experimental values. Table 3 provides a comprehensive catalog of all composite values. The anomalies observed in the thermodynamic acoustic excess parameters, V^E and K_s^E, are depicted in Figure 3 and Figure 4, respectively. As the temperature increases, the

excess parameters decrease due to thermal agitation in all fluids [19].

For high concentrations of 2MCH, the values of V^E are positive or slightly negative, but the trend becomes negative as the concentration of [BMPip]BF_4 increases in the respective composites. The negative flip sharpness of V^E is clearly visible in Figure 3, indicating the formation of stronger H-bonds at higher concentrations and weaker H-bonds at lower concentrations of composites. Furthermore, the formation of H-bonds is very weak at high concentrations and higher temperatures [20].

The abnormality in excess isentropic compressibility at all temperatures is illustrated in Figure 4, covering the entire concentration range of all composites. The K_s^E values are consistently negative for all investigated temperatures and composites. The negative sign of K_s^E is crucial in evaluating the compactness resulting from molecular interactions in multi-component mixtures, indicating interstitial accommodation and oriental ordering that contribute to a more compact structure.

Fort and Moore [21] suggested that binary fluids with distinct molecular sizes and shapes mix well, leading to a reduction in volume and negative values of K_s^E. This negative K_s^E value is clearly evident in Figure 4, indicating greater steric hindrance in the formation of hydrogen bonds in the respective composites.

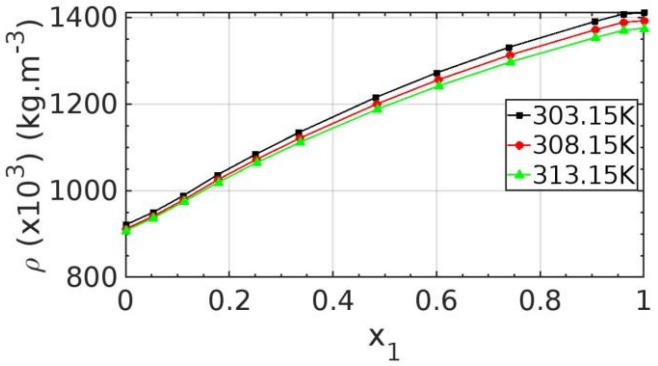

Figure 1: Plot of thermo physical features of density versus molefraction

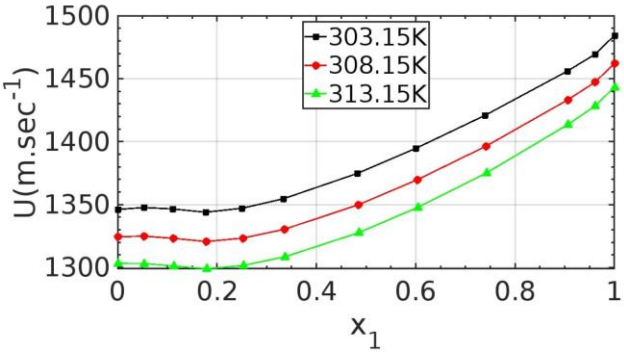

Figure 2: Plot of thermo physical features of speed of sound versus molefraction

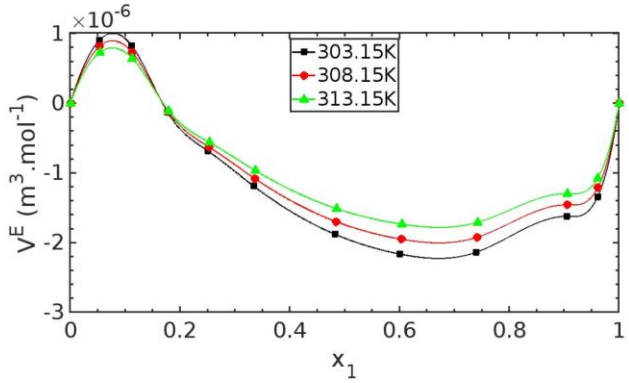

Figure 3: Plot of thermo physical features of excess volume versus molefraction

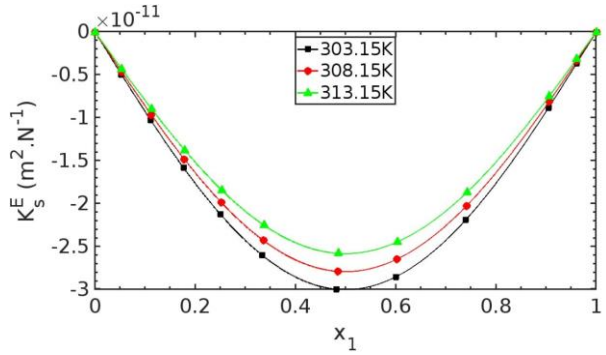

Figure 4: Plot of thermo physical features of excess isentropic compressibility versus molefraction

3.2 Reduced Redlich-Kister Polynomial Analysis

The Redlich-Kister approach, although inevitable, occasionally misguides different composites, particularly in the low concentration regions. To address these issues and provide more specific insights into composites, Desnoyers[22] proposed the effective Reduced Redlich-Kister (RRK)[23] polynomial analysis. This analysis offers an equation that is equivalent to the apparent molar quantity of respective excess parameters across the entire concentration range. So the equation becomes

$$Q_{Y_{RRK}^E}(x_1) = \frac{Y_{RK}^E(x_1)}{x_1(1-x_1)} --(6)$$

While excess thermodynamic quantities show flipping signs, sharpness, and magnitude of differences in composites, the RRK polynomial specification highlights promising features for understanding the origin of dissimilar solutions. The abnormalities of $Q_{V_m^E,T}(x_1)$ at all temperatures are illustrated in Figure 5 for all composites and concentrations. These values demonstrate higher attributes at low temperatures.

This distinction clearly indicates the presence and strength of hydrophobic interactions in the higher concentration region of IL. Conversely, hydrophobic interactions are very weak at high concentrations of 2MCH. In the present scenario, the reduced function values exhibit higher values on the 2MCH side and lower values on the IL side.

The abnormalities of $Q_{K_S^E,T}(x_1)$ at all temperatures are illustrated in Figure 6 for all composites and concentrations. This is clearly representing the replicated sequence. This result suggests that the composites are less compressible than ideal mixtures, indicating strong interactions within these composites. It also indicates that 2MCH molecules experience more steric hindrance from IL molecules at 303.15K.

3.3 Partial molar volumes and partial molar isentropic compressibilities

The RRK functions of $Q_{V_m^E,T}(x_1)$ and $Q_{K_S^E,T}(x_1)$ at infinite dilution, with constant temperature and pressure, serve as additional tools to represent partial molar volumes[24] and partial molar isentropic compressibilities. The modified expression for the above extrapolation (Equation 6) becomes:

$$Q_{V_m^E}(x_1 = 0) = A_{0,T} - A_{1,T} + A_{2,T} - A_{3,T} = \bar{V}_{1,p,m}^{E,\infty} = \bar{V}_{1,p,m}^{\infty} - V_{1,m} - -(7)$$

$$Q_{V_m^E}(x_1 = 1) = A_{0,T} + A_{1,T} + A_{2,T} + A_{3,T} = \bar{V}_{2,p,m}^{E,\infty} = \bar{V}_{2,p,m}^{\infty} - V_{2,m} - -(8)$$

Here, $\bar{V}_{1,p,m}^{E,\infty}$ and $\bar{V}_{2,p,m}^{E,\infty}$ are the excess pure molar volumes of the two components, IL and 2MCH, respectively. And also, $\bar{V}_{1,p,m}^{\infty}$ and $\bar{V}_{2,p,m}^{\infty}$ are the pure molar volumes of the two components, IL and 2MCH, respectively. Further, $V_{1,m}$ and $V_{2,m}$ are pure molar volumes of two components IL and 2MCH, respectively. Similarly, the equations analogy holds true for partial molar isentropic compressibilities. However, the real partial molar volumes and partial molar isentropic compressibilities with respect to a mole fraction at constant pressure and temperature can be evaluated using the following differential equation:

$$\bar{V}_{i,p,m} = V_m(x_i) - x_j\left(\frac{\partial V_m(x_j)}{\partial x_j}\right)_{T,P} - -(9)$$

$$\bar{K}_{i,p,s} = K_s(x_i) - x_j\left(\frac{\partial K_s(x_j)}{\partial x_j}\right)_{T,P} - -(10)$$

Here x_i and x_j are the mole fractions of the two components in the composite (i=1,2 & j=i-1). The intermolecular interactions in the composites can be interpreted in terms of the packing efficiency of molecules with the help of partial molar volumes and partial molar isentropic compressibilities. The partial molar volumes of the two components $\bar{V}_{1,p,m}$ and $\bar{V}_{2,p,m}$ play a vital role in binary fluids as the influence of the components in the mixtures changes with respect to composition concentrations and temperature. Figure 7 illustrates the partial molar volumes of all components.

In this figure, the scaffold Z symbol graph consists of three styled lines representing solid lines ($\bar{V}_{1,p,m}$), dashed lines (total molar volume, V), and dotted lines ($\bar{V}_{2,p,m}$). For all combinations, the partial molar volumes of both components, $\bar{V}_{1,p,m}$ and $\bar{V}_{2,p,m}$, are lower than their individual values in the pure state, indicating a decrease in the influence of individual components in their respective lower concentration regions. The abnormalities are examined for all constant temperature intervals, suggesting the presence of solute-solvent interactions between unlike molecules. Hence, from the representation in Figure 7, the effect of domain influence of volume is low at 303.15K compared to other two temperatures.

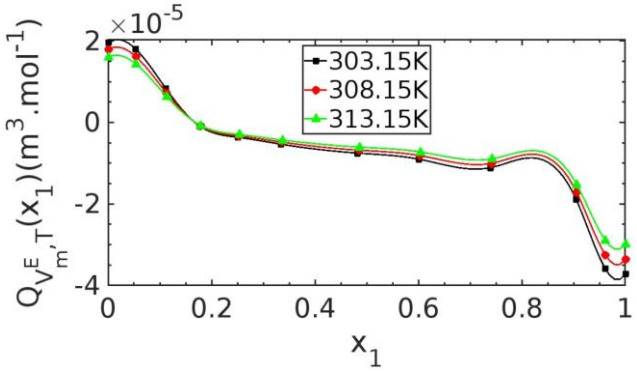

Figure 5: Plot of thermo physical features of reduced excess volume versus molefraction

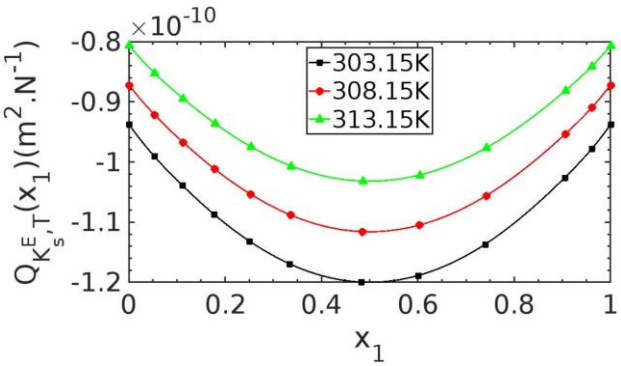

Figure 6: Plot of thermo physical features of reduced isentropic compressibility versus molefraction

Table 3: Coefficients of redlich-kister equation parameters and standard deviations at different temperatures.

Combination	T/K	Redlich-kister equation coefficients				error
		$A_{0,T}$	$A_{1,T}$	$A_{2,T}$	$A_{3,T}$	$\sigma(Y_{RK}^E)$
V_m^E (10^{-6} $m^3.mol^{-1}$)						
IL(1) + 2MCH(2)	303.15	-7.2423	1.0750	-1.8174	-29.455	0.2671
	308.15	-6.6055	0.6553	-1.2119	-25.689	0.2277
	313.15	-5.8993	0.8973	-1.0367	-23.736	0.2100
K_s^E (10^{-11} $m^2.N^{-1}$)						

IL(1) + 2MCH(2)	303.15	-5.4681	-15.832	23.509	116.09	4.8210
	308.15	-153.87	-4771.1	-18.477	7651.7	20.951
	313.15	-18.956	-37.622	13.478	54.30	2.2414

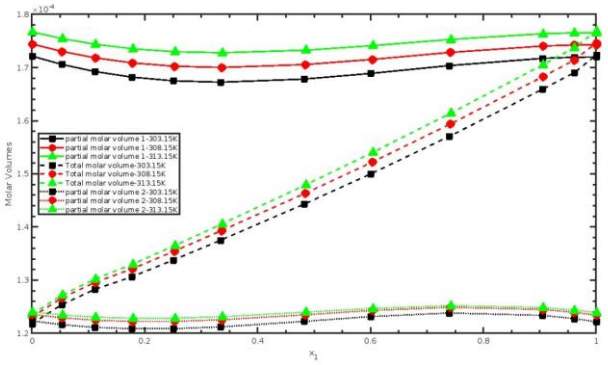

Figure 7: Plot of partial molar volumes against molefraction and temperature for the solution [BMPip]BF_4(1)+2MCH(2).

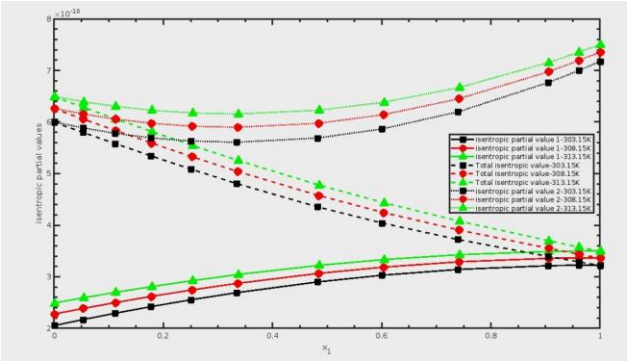

Figure 8: Plot of partial molar isentropic compressibilities against molefraction and temperature for the solution [BMPip]BF_4(1)+2MCH(2)

The partial isentropic compressibilities of two components $\overline{K}_{1,p,s}$ and $\overline{K}_{2,p,s}$ are also play crucial role in binary mixture. Because the geometrical influence of the components in the mixture changes with respect to the composition concentration and temperature. In this scenario, the partial isentropic compressibilities of components [BMPip]BF_4+2MCH have been shelled in Figure 8. In this figure, the mirror scaffolded inverted Z symbol graph contains three styled lines, which are concerned to solid lines ($\overline{K}_{1,p,s}$), dashed lines (total isentropic compressibility, K_s) and dotted lines ($\overline{K}_{2,p,s}$). The partial isentropic compressibilities $\overline{K}_{1,p,s}$ and $\overline{K}_{2,p,s}$ are less at 303.15K. This clearly suggests the breaking of dipole inclusions in [BMPip]BF_4+2MCH at 303.15K has more than compared to the other higher temperatures in that combination.

4. Conclusions

In this comprehensive framework, meticulous calibration of the values of excess thermodynamic parameters has been undertaken for the entire composition of IL+2MCH, encompassing a wide range of temperatures. This rigorous calibration procedure effectively reveals the unequivocal presence of robust hydrogen bonding and dipole-inclusion interactions within the constituent molecules. Moreover, to delve deeper into the intricate nature of these interactions, an innovative and cutting-edge approach utilizing the contemporary RRK polynomial has been employed. This powerful analytical tool allows for the precise determination and elucidation of the reduced excess thermodynamic parameters across the entire composition spectrum, faithfully capturing the subtleties and nuances of the system under investigation.

Remarkably, this comprehensive analysis shines a spotlight on a remarkable phenomenon—the inherent steric hindrance experienced by the 2MCH molecules, owing to their smaller molar mass, when in the presence of the larger molar mass of IL at the corresponding temperatures. This insightful revelation opens new vistas of understanding and uncovers the intricate interplay between molecular characteristics and their impact on the overall behavior of the system.

As the temperatures ascend, an intriguing trend emerges the reduced excess parameters exhibit a discernible decrease. This captivating behavior can be attributed to the escalating thermal agitations within the compositions, which gradually weaken the molecular interactions and consequently modulate the system's thermodynamic landscape.

To provide a holistic perspective on the system, the partial molar volumes and partial molar and isentropic compressibilities of all components have been meticulously mapped and presented in an immersive scaffold format. This visually captivating representation allows for a profound appreciation of the profound intermolecular interactions that govern the IL(1)+2MCH(2) composite at the distinctive temperature of 303.15K, surpassing the levels observed at other higher temperatures. This captivating insight highlights the temperature-dependent dynamics of the system and provides further evidence of the intriguing interplay between molecular species within the composite matrix.

In essence, this rigorous and comprehensive analysis, fortified by cutting-edge methodologies and effective analytical tools, unveils a wealth of invaluable information about the intricate thermodynamic behavior of the IL+2MCH composite. It offers profound insights into the molecular intricacies, shedding light on the intermolecular forces and interactions that shape the overall thermodynamic landscape.

References

[1] R. Umapathi, S.B. Vepuri, P Venkatesu and M.E. Soliman, “Comprehensive computational and

experimental analysis of biomaterial toward the behavior of Imidazolium-based ionic liquids: An interplay between hydrophilic and hydrophobic interactions", Journal of physical chemistry B, Vol.121, pp.4909-4922, April 2017. Doi: 10.1021/acs.jpcb.7b02208.

[2] H. Passos, M.G. Freire and J.A.P. Coutinho, "Ionic liquid solutions as extractive solvents for value added compounds from biomass", *Green Chemistry*, Vol.16, pp. 4786-4815, July 2014. Doi: 10.1039/c4gc00236a.

[3] P. Suneetha, T. S. Krishna, M. Gowarisankar, K. Ravindhranath and D. Ramchandran, "Molecular interaction between binary mixtures 1-butyl -3-methyl-imidazolium bis (trifluoromethylsulfonyl) imide with N-Vinyal-2-pyrrolidine at different temperatures", *Journal of Chemical Thermodynamics*, Vol.108, pp.181-192, May 2017. Doi:10.1016/j.jct.2017.01.014.

[4] K. Nekkala, V. Shanmukha Kumar, D. Ramchandran, "Development and validation for the simulataneous estimation of lamivudine, teneofovir disproxyil dolutegravir in drug product by RP-HPLC", *Journal of Pharmaceutical Sciences and Research*, Vol.9,pp.1505-1510, 2017.

[5] Y.V.S. Kumar, U.R. Mallu, I.V.K. Viswanath, D. Balasubramanyam and G.N. Murthy, "A novel rapid resolution high performance liquid chromatographic related substance method development and validation of levetiracetam in bulk drug manufacturing of Active pharmaceutical ingredient", *Journal of Pharmaceutical Sciences and Research,*Vol. 9, pp.1511-1521, 2017.

[6] U.R.Mallu, V.R.Anna and B.B. Kasimala, "Rapid stability indicating HPLC method for the analysis of leflunomide and its related impurities in bulk drug and formulations", *Turkish Journal of Pharmaceutical Sciences*, Vol.16, pp.457-465, August 2019. doi. 10.4274/tjps.galenos.2018.34635

[7] B.B. Kasimala, A.V. Rao and U.R. Mallu, "Stability indicating reversed-phase HPLC method for the separation and estimation of related impurities of Cilnidipine in pharmaceutical formulations", *Indian Drugs*, Vol.55, pp.41-49, December 2018.

[8] A.V. Rao, B.R. Kumar and S.D.R. Rao, "Structural, micro structural and electrochemical studies on $LiMn_{2-x}(GdAl)_xO_4$ with spinel structure as cathode material for Li-ion batteries", *Ceramics International*, Vol.44, pp.15116-15132, September 2018. Doi: 10.1016/j.ceramint.2018.05.148.

[9] A. Rajkamal and T. Ranjit, "Carbon Allotropes as anode material for lithium-ion batteries" *Advanced Materials Technologies,*Wiley online library, Vol.4,August2019. Doi: 10.1002/admt.201900307.

[10] R.R. Samal, B. Dash, C.K. Sarangi, K. Sanjay, T. Subbaiah, G. Senanayake and M. Minakshi, "Influence of sunthesis temperature on growth and surface morphology of Co_3O_4 nanocubes for supercapacitor applications", *Nanomaterials*, Vol.7, pp.356-368,October2017. Doi:10.3390/nano7110356.

[11] N.K. Jyothi, K.V. Kumar, G.S. Sundari and P.N. Murthy, " Ionic conductivity and battery characteristic studies of new PAN-based Na^+ ion conducting gel polymer electrolyte system", *Indian Journal of Physics,*Vol.90, pp.289-296, August 2016. Doi: 10.1007/s12648-015-0758-9.

[12] G. V. Gangadhara Rao, Shaik Babu, T. Kalimulla and K. Govinda Rao, "Intermolcular interaction studies of binary liquid mixtures of 2-methoxy cyclohexanone with o-anisidine/m-anisidine/p-anisidine in terms of of thermoacoustic parameters at different temperatures" *Indian Journal of Pure and Applied Physics*,Vol.58, pp.657-666, September 2020.

[13] E. D. Morgan, "Vogel's textbook of practical organic chemistry, Endeavour", 5th ed. 1990. Doi: 10.1016/0160-9327(90)90017-l.

[14] M.G. Sankar, V.Ponneri, K.S. Kumar, Sivarambabu Sakamuri "Molecular interactions between amine and cyclic ketones at different temperatures", *Journal of Thermal Analysis and Calorimetry*, Vol.115, pp.1821-1827, October 2013. DOI: 10.1007/s10973-013-3312-z

[15] G. V. Gangadhara Rao and Shaik Babu,"Molecular Interactions of Piperidinium based ionic liquids with water/Alcohol at different temperatures", *Asian journal of chemistry*, Vol.33, pp.195-202, October 2020. https: //doi.org/10.14233/ajchem.2021.22977.

[16] O. Redlich and A.T. Kister, "Algebric representation of thermodynamic properties and the classification of solutins", *Industrial Engineering of Chemistry*, Vol.40, pp.345-348, February 1948. Doi: 10.1021/ie50458a036.

[17] B. Mahaboob, B. Venkateswarlu, K.A. Azmath, C. Narayana and J.P. Praveen, "On OLSestimation of stochastic linear regression model", *International Journal of Scientific and Technology Research*, Vol.8, pp.1-3, August 2019.

[18] D.P. Kumar and K. Rajyalakshmi et al, "Analysis of mobile technology switching behavior of consumer using

chi-square technique: a model study from hyderabad", *International Journal of Civil Engineering and Technology*, vol.8, pp.99-109, 2017.

[19] T. Vishwam, K. Parvateesam, S. Babu, S.S. Sastry and V.R.K. Murthy, "Study of excess dielectric relaxation spectroscopy study of propylene glycol/ethanol binary mixtures: temperature dependence", *Indian Journal of Pure and Applied Physics*, Vol.54, pp.597-611, September 2016.

[20] S.S. Sastry, B. Shaik, T. Viswam and H.S. Tiong, "Excess thermodynamic and acoustic properties for the binary mixtures of methyl benzoate at T=(303,308,3123, 318 and 323)K", *Physics and Chemistry of Liquids*, Vol.52, pp. 272-286, August 2014. Doi: 10.1080/00319104.2013.820302.

[21] R.J.F. and W.R. Moore, "Visccosities of binary liquid mixtures", *Transactions of the faraday Society*, Vol.62, pp.1112-1119, 1966.

[22] J.E. Desnoyers and G. Perron, "Treatment of excess thermodynamic quantities for liquid mixtures", *Journal of Solution Chemistry*, Vol.26, pp.749-755, August 1997. Doi: 10.1007/BF02767781.

[23] D. Das, A. Messasdi, Z. Barhoumi and N. Ouerfelli, "The relative reduced redlich-kister equations for correlating excess properties of N-n-dimetthylacetamide+water binary mixtures at temperatures from 298.15K to 318.15K", *Journal of Solution Chemistry*, Vol.41, pp.1555-1574, October 2012. Doi: 10.1007/s10953-012-9878-2.

[24] R. Trabelsi, S. Babu, H. Salhi, N. Ouerfelli and A. Toumi, "Investigation of the reduced redlich-kister excess properties of 1,4-dioxane+isobutyric acid binary mixtures at temperatures from 295.15 to 313.15K", *Physics and Chemistry Liquids*, Vol.56, pp.801-815, November 2017. Doi: 10.1080/00319104.2017.1399267.